Mixing Mechanics of Three-Dimensional Rectangular Jet

Il Won Seo[1] and Seok Jae Kwon[2]

1. INTRODUCTION

The plane jet assuming the infinite slot width has been analyzed through the two-dimensional concept that is frequently adopted to describe the dynamics of the multi-jet widely used for industrial and domestic wastes (Fig. 1). However, since most plane jets are discharged from the rectangular slot with a finite width and height, the study of mechanics of a rectangular jet requires better understanding of the three-dimensional process of the jet growing by entrainment of surrounding fluids. The aspect ratio(AR) for a rectangular slot with a finite width L, and height, B, can be defined as the slot width divided by the slot height (L/B). The previous experimental observations on the velocity field for the non-buoyant three-dimensional slot jet indicate that flow zones can be divided into three distinct regions: potential core region, two-dimensional region, and axisymmetric region as shown in Fig. 1 (Sforza *et al.*, 1966).

Among the studies of two-dimensional and axisymmetric water jets, only a few investigations (Demissie, 1980) dealt with three-dimensional water jets. In this study, a comparison between the results of the present study and theoretical equations has also been made in an attempt to understand the behavior of jet flows in more detail. This investigation also provides the three distinct regions based on the experimental results of the mean velocity fields measured by particle image velocimetry.

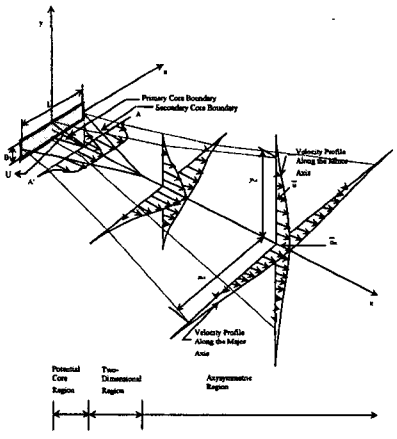

Fig. 1. Schematic Diagram of 3-D Rectangular Jet

2. RESEARCH BACKGROUNDS

The maximum velocity was found to vary in different manner in three regions. In the two-

[1] Prof., Dept. of Civil Engineering, Seoul National University, E-mail: seoilwon@plaza.snu.ac.kr

[2] Grad. Student, Dept. of Civil Engineering, Seoul National University, E-mail: sj79kwon@chollian.net

dimensional region, the axial velocity is inversely proportional to $x^{-1/2}$ (x is the Cartesian coordinate to the longitudinal jet direction) while it is inversely proportional to x^{-1} for the axisymmetric region in a similar manner (Daily and Harleman, 1966).

For an elemental source of area, dA, the expression based on the point source concept can be expressed as

$$\frac{\bar{u}_m^2}{U^2} = \frac{dA}{\pi b^2} \tag{1}$$

where $\bar{u}_m$ is the mean centerline velocity, U is the exit velocity, b is a length scale($b=cx$) for an axisymmetric jet, and c is an experimental coefficient. As the governing equation is linear, the principle of superposition can be adopted to find the resultant dynamic pressure at a certain point. Along the centerline of the jet, $y=0$ and $z=0$ (y and z are the Cartesian coordinates along the minor and major axes, respectively), thus, the centerline velocity distribution can be expressed as

$$\frac{\bar{u}_m^2}{U^2} = erf\left(\frac{B}{2b}\right) erf\left(\frac{L}{2b}\right) \tag{2}$$

In this equation, $c=0.105$ obtained by Hongwei(2000) for a axisymmetric jet was substituted to provide the centerline velocity profile for the three-dimensional rectangular jet.

3. EXPERIMENTS

The experiments have been carried out in a glass-walled rectangular tank that is 6.0 m long, 1.2 m wide, 1.0 m high as shown in Fig. 2. Aspect ratios of 5, 10, and 20 are obtained by making three pairs of inserts with widths of 5.0, 3.5 and 2.5 mm, respectively. In this study, particle image velocimetry (PIV) system was used to measure the velocity profiles. The experimental conditions of typical cases conducted in terms of the aspect ratios of 5, 10 and 20 in this study are listed in Table 1.

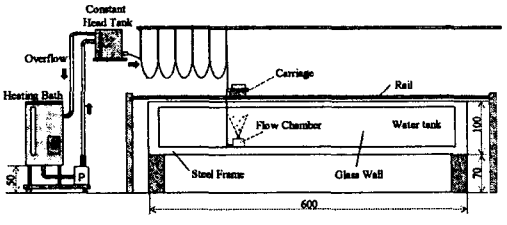

Fig. 2. Schematics of Experiments (Unit : cm)

Table 1. Experimental Conditions

Aspect Ratio	Axis	Case	U(cm/s)	Re_j ($=UB/\nu$)	F_j ($=U/\sqrt{gB}$)
5	Major Axis	AR5-150MAJC	33.33	1667	1.51
	Minor Axis	AR5-150MINC	33.33	1667	1.51
	Major Axis	AR5-200MAJC	44.44	2222	2.01
	Minor Axis	AR5-200MINC	44.44	2222	2.01
10	Major Axis	AR10-200MAJC	45.35	1587	2.45
	Minor Axis	AR10-200MINC	45.35	1587	2.45
	Major Axis	AR10-250MAJC	56.69	1984	3.06
	Minor Axis	AR10-250MINC	56.69	1984	3.06
20	Major Axis	AR20-150MAJC	33.33	833	2.13
	Minor Axis	AR20-150MINC	33.33	833	2.13
	Major Axis	AR20-200MAJC	44.44	1111	2.84
	Minor Axis	AR20-200MINC	44.44	1111	2.84

[Remarks] Re_j=Reynolds Number, ν=Kinematic Viscosity, F_j=Densimetric Froude Number

4. RESULTS

Fig. 3 shows the instantaneous images captured by CCD camera along the minor and major axes for the aspect ratio of 10. Fig. 4 provides the lateral velocity distribution measured at different axial distances on the center sections (z=0) of the minor and major axes for the aspect ratio of 10. It is observed that the centerline velocity of each section decreases. The lateral velocity profile along the major axis shows the double peak distribution called "saddle-back" distribution seems to be more dominant as the aspect ratio increases.

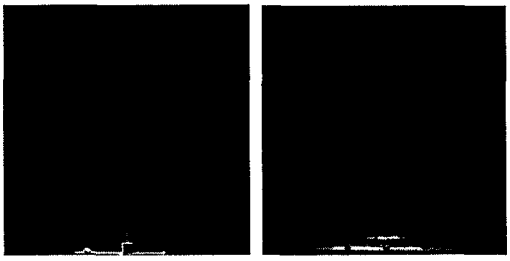

(a) AR10-250MINC (b) AR10-250MAJC

Fig. 3. Instantaneous Images for AR of 10

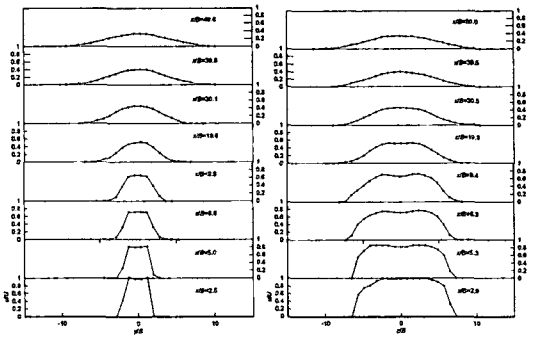

(a) AR10-250MINC (b) AR10-250MAJC

Fig. 4. Lateral Velocity Profiles (AR:10)

The centerline velocity for three-dimensional rectangular jets has three distinct regions with transition zones from one region to another. Fig. 5 shows the longitudinal variation of the centerline velocity and three distinct regions of the rectangular jet for the aspect ratios of 5, 10, and 20. It is seen that the theoretical result from Eq. (2) is in generally good agreement with the measured centerline velocity.

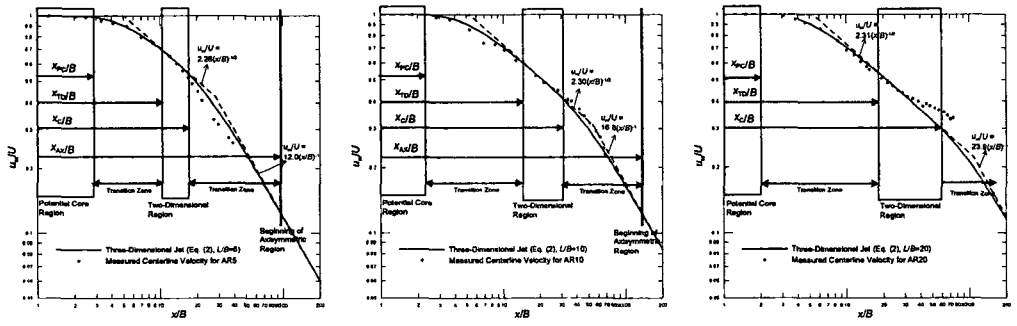

(a) AR5 (b) AR10 (c) AR20

Fig. 5. Division of the Three Distinct Regions of the Rectangular Jet

The jet half widths($=y_{1/e}$) along the minor axis are determined from the Gaussian distributions fitted to the velocity profiles while the half width($=z_{1/e}$) along the major axis is determined by visually fitting a curve through the data points. Fig. 6 shows the variation of the

jet half-widths, $y_{1/e}/B$ and $z_{1/e}/B$, for L/B = 5, 10, and 20.

The spreading rates on the minor axis tend to gradually and slightly decrease on the basis of the end of the two-dimensional region. This implies that the spreading rates for the rectangular jet should be described in terms of the two-dimensional and axisymmetric zones, recpectively. The overall spreading rate in the two-dimensional region for the aspect ratios of 5, 10, and 20 is estimated to be 0.125 which is close to the value of 0.12 proposed by Papanicolaou and List (1988). The jet half width on the major axis decreases initially and begins to increase with longitudinal distance.

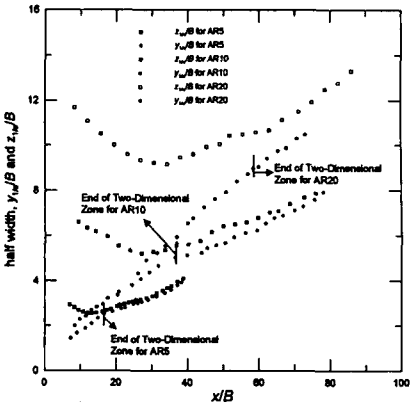

Fig. 6. Half-Widths $y_{1/e}/B$ and $z_{1/e}/B$

5. CONCLUSIONS

This study has investigated the behavior of nonbuoyant and turbulent three-dimensional rectangular water. The theoretical centerline velocity from Eq. (2) shows generally close agreement with the measured centerline velocity. The experimental result of the centerline velocity decay shows the division of the three distinct regions. The spreading rates on the minor axis tend to decrease on the basis of the end of the two-dimensional region in which the overall spreading rate is estimated to be 0.125.

6. REFERENCES

Daily, J. W., and Harleman, D. R. F. (1966). *Fluid Dynamics*, Addison-Wesley Publishing Company, Inc.

Demissie, M. (1980). "Diffusion of Three-Dimensional Slot Jets With Deep and Shallow Submergence." Doctor of Philosophy in Civil Engineering, University of Illinois, Urbana-Champaign, USA.

Hongwei, W. (2000). "Investigations of Buoyant Jet Discharges Using DPIV and PLIF.' Doctor of Philosophy in Civil & Structural Engineering, Nanyang Technological University, Singapore.

Papanicolaou, P. N., and List, E. J. (1988). "Investigations of Round Vertical Turbulent Buoyant jets." *Journal of Fluid Mechanics*, 195, 341-391.

Sforza, P. M., Steiger, M. H., and Trentacoste, N. (1966). "Studies on Three-dimensional Viscous Jets." *American Institute of Aeronautics and Astronautics Journal*, 4(5), 800-806.